SOME CONSIDERATIONS IN THE CANFLEX-NU FUEL DESIGN[1]

K-S. Sim and H.C. Suk
(Korea Atomic Energy Research Institute)

M. Tayal, P. Alavi, I.E. Oldaker and J.H. Lau
(Atomic Energy of Canada Limited)

ABSTRACT

The CANDU Flexible-natural uranium (CANFLEX-NU) fuel bundle is being developed as the next logical evolution of CANDU fuel. Several design details of the CANFLEX bundle differ from the current 37-element fuel bundle. For example, the CANFLEX bundle uses buttons that enhance critical heat flux, smaller element diameters, and thinner sheaths. These changes contribute to the many advantages offered by the CANFLEX bundle. Nonetheless, the impact of these modified parameters on fuel failure mechanisms must be examined. For example, smaller diameter may lead to increased potential for flow-induced vibration and fatigue. Similarly, thinner sheaths may potentially lead to increased likelihood of collapse of the sheath into concentrated axial gap in the element due to the coolant pressure. Likewise, thin sheath and altered pellet dimensions may also potentially influence the defect threshold for stress-corrosion cracking during power ramps. The fatigue behaviour of the element may be different from the standard 37-element bundle under the condition of the significant number of power cycles. As part of the design verification of the CANFLEX bundle, the above failure mechanisms were analysed using well-established methods with reasonable support from relevant experiments or operating experience. As the analysis results show, the CANFLEX-NU fuel bundle is expected to exhibit excellent integrity during its lifetime in the reactor.

INTRODUCTION

The CANFLEX fuel bundle with natural uranium fuel, known as CANFLEX-NU, is being developed jointly by AECL and KAERI, and is now at the stage of final design verification. Verification of the design of the CANFLEX fuel bundle is performed in a way that shows that design criteria are met, and is mostly covered by proof tests such as flow and irradiation tests. However, some design parameters are verified by analyses rather than by experiments because appropriate experimental simulations are unavailable in some areas or because they take a long time to provide results. This paper discusses some design parameters of the CANFLEX-NU fuel bundle that have been verified by analyses rather than by experiments. The next paragraph outlines the parameters that are of prime interest in this paper.

[1] Presented at the Fifth International Conference on CANDU Fuel, Canadian Nuclear Society, Toronto, Canada. 1997 September 21-25.

The CANFLEX fuel bundle is composed of 43 elements of two sizes. Of these, 35 are small-diameter elements that are located in the two outer rings. As a result, the peak element ratings of the bundle are reduced by 20% compared with the peak element ratings of the standard 37-element bundle. Despite this good performance, the small-diameter elements may show greater flow-induced vibration due to the axial flow of the coolant, compared to the 37-element bundle. This could lead to fatigue failure at the weld between the endcap and endplate, or in the endplate webs. To maintain good neutron economy, a thin-walled sheath was chosen for the small-diameter elements. This design feature, along with the differences in pellet dimensions, may have potential for stress-corrosion cracking (SCC) failure due to power ramps. Sometimes, the axial gap is not evenly distributed in both ends of the element and among pellets but is concentrated in one end of the element. Collapse of the sheath into the concentrated axial gap in the element due to the external coolant pressure is also of interest because of the thin-walled sheath. The thin wall tubing and lower element ratings may lead to different mechanical behaviour of the element from the standard element and result in different fatigue behaviour under the condition of a significant number of power cycles.

FATIGUE ANALYSIS FOR CANFLEX-NU ENDPLATE

Fuel bundles in CANDU 6 reactors are cooled by heavy-water coolant which is forced to flow at a high velocity of about 9 m/s. As a consequence, flow-induced lateral vibration of the element occurs in this axial flow, and the potential for fatigue at the weld between the endcap and the endplate, or in the endplate webs, must be considered.

Analysis Model

Stress Equations

Tayal and Choo [1] extended the classical elasticity theory and developed a method for assessing the influence of lateral vibrations of a fuel element on the endplate stresses. Their model was derived with the assumption that the element is represented as a beam with a uniformly distributed load that is supported at both ends by torsional springs representing the endplates. This model is used here for the analysis of the CANFLEX-NU endplate stresses (for a detailed discussion and equations, see reference [1]).

The flexural rigidity of an element is calculated by considering the element as a composite beam comprising of the sheath and the pellet: Tight radial contact is expected between the pellet and the sheath during reactor operation because of the thermal expansion of the pellet and the coolant pressure on the sheath. The UO_2 pellet is likely cracked, even at very small levels of tensile stress; therefore, the neutral axis for the bending of the element is not the same as the geometric centreline of the element. In the classical approach of elastic bending, the location of the neutral axis (η) from the geometric centre, is determined by balancing the compressive and tensile forces. This leads to the following equation:

$$E_p A_p y_p - E_s A_s \eta = 0 \qquad (1)$$

Similarly, the flexural rigidity of the fuel element is determined by summing the contributions to the local bending moment by the pellet and the sheath, and then relating it to the net curvature at the cross-section. This gives the following equation for the flexural rigidity of the composite beam comprising of the sheath and the pellet:

$$EI = E_p\left(I_p + A_p y_p^2\right) + E_s\left(I_s + A_s \eta^2\right) \tag{2}$$

where E, A and I represent modulus of elasticity, cross-sectional area and moment of inertia, respectively. Subscripts p and s represent pellet and sheath, respectively. As illustrated in Figure 1, η is the distance of the neutral axis of an element from its geometric centre, and y_p is the centroid distance of the segment of solid circle which simulates the compressive part of the UO_2 pellet. The sheath inside radius is R_1 and the angle of the segment of the solid circle is 2α. The parameters in Equations (1) and (2) are calculated by Roark's formula [2], as given below:

$$\begin{aligned}
A_p &= R_1^2\left(\alpha - \sin\alpha\ \cos\alpha\right) \\
y_p &= R_1\left[\frac{2\sin^3\alpha}{3\left(\alpha - \sin\alpha\ \cos\alpha\right)} - \cos\alpha\right] \\
I_p &= \frac{R_1^4}{4}\left[\alpha - \sin\alpha\ \cos\alpha + 2\sin^3\alpha\cos\alpha - \frac{16\sin^6\alpha}{9\left(\alpha - \sin\alpha\cos\alpha\right)}\right] \qquad \text{for } \alpha > \frac{\pi}{4}
\end{aligned} \tag{3}$$

$$\begin{aligned}
A_p &= \frac{2}{3}R_1^2\,\alpha^3\left(1 - 0.2\,\alpha^2 + 0.019\,\alpha^4\right) \\
y_p &= 0.2\,R_1\alpha^2\left(1 - 0.0619\,\alpha^2 + 0.0027\,\alpha^4\right) \\
I_p &= 0.01143\,R_1^4\,\alpha^7\left(1 - 0.349\,\alpha^2 + 0.0450\,\alpha^4\right) \qquad \text{for } \alpha < \frac{\pi}{4}
\end{aligned} \tag{4}$$

Vibration Amplitude

As described above, the moment and stress in the endplate are significantly dependent on the lateral deflection of the element. The lateral deflection is considered here as the amplitude of the flow-induced vibration due to the axial flow of the coolant.

Païdoussis [3] derived a model to predict the lateral amplitude of vibration, δ, for a cylinder subjected to axial flow.

$$\delta = A_v / D$$

$$= a^{-4} \frac{\left(u^2 \, Re \, \varepsilon^2\right)^{4/5}}{1 + 2u^2} \left(\frac{\beta^{2/3}}{1 + 4\beta}\right) \left(1 \times 10^{-5}\right)$$

where $$a = \left[\frac{(m + M) \, L^4}{EI}\right]^{1/4} \omega^{1/2}$$

and was given as 4.73 for the cylinder fixed at both ends,

A_v = the lateral amplitude of vibration of the element,
D = the diameter of the element,
L = the length of the element,
M = the mass of the flow per unit length $= \pi D^2 \rho / 4$,
m = the mass of the fuel element per unit length,
ω = the circular frequency of oscillation of the fuel element at zero flow,
u = dimensionless flow velocity $= UL\left(\frac{M}{EI}\right)^{1/2}$
U = the average velocity of the axial flow,
Re = Reynolds number,
ε = L / D,
β = $\frac{M}{M + m}$
ρ = the density of the flow.

Calculated Results and Discussions

Validation of the Païdoussis Correlation for Application to CANFLEX Fuel Elements

The Païdoussis correlation was adapted to the results of the CANFLEX fuel element excitation tests which were conducted in axial flow in an air-water mixture. From the database of the CANFLEX element excitation test, some measurements in the range of Reynolds number greater than 10^5 and void fraction (x) less than 50% were selected for the validation of the Païdoussis correlation. The selected measurements cover the hydraulic conditions of CANDU 6. The comparative results between the measurements and the predictions showed good agreement, as represented in Figure 2. The average difference was -0.7%. This result indicates that the Païdoussis model predicts very well the lateral amplitude of vibration of CANFLEX fuel elements subjected to axial coolant flows.

Fatigue Analysis of the CANFLEX Endplate

This assessment addresses fatigue of the endplate due to lateral vibration of the fuel element. The midplane deflections of the small-diameter and large-diameter elements were predicted as 53 μm and 45 μm, respectively, by the Païdoussis correlation given by Equation (5). These were obtained without consideration of restraints from spacers. To take into account the restraints imposed by spacers, the predicted midplane deflection was compared to the maximum spacing between matching spacers and corrected appropriately. With the consideration of the restraints, the midplane deflections were 53 μm for the outer element, 22 μm for the intermediate element, 21 μm for the inner element and 42 μm for the centre element. For the calculation, conservative values were applied to the parameters affecting the vibration amplitude of the element; that is, Re = 5.8×10^5 and U = 9.6 m/s.

For the stress analyses of the endplate weld, the weld diameter was assumed to be the same as the width of the endplate ring. The highest stress at any endcap-endplate weld was calculated to be 18 MPa. This occurred in the centre element even though the midplane deflection was highest in the outer element. The centre element is welded to the centre rib of the endplate, and the width of the rib is smaller than that of the ring on which other ring elements are welded. Therefore the centre element has the smallest weld diameter which in turn leads to the highest weld stress. This maximum weld stress is lower than the appropriate fatigue limit as discussed below.

Tayal and Choo [1] suggested the fatigue strength of the endplate weld as 22 MPa. Below this level fatigue failure is not expected at this weld. The fatigue strength (i.e., endurance limit) of Zircaloy depends in part on the residual stress. The value of residual stress in the endplate weld is not known, but welding can generate local residual stresses up to the yield strength. It was assumed that the initial residual stress in the endplate weld is equal to the yield strength. Under the operating temperature and neutron flux of the reactor, stress relaxation is expected to rapidly reduce the initial residual stress. But for conservatism, it was also assumed that the residual stress maintains its initial high value. Further, a safety factor of 2 was applied to cover the effects of specimen size, environment and surface finish. Under the above assumptions, Tayal and Choo determined the fatigue strength from O'Donnell and Langer's curves for the endurance limit of Zircaloy for 1 million cycles at 300°C to be 55 MPa. A reduction in fatigue strength is possible because the sharp reduction of the fuel element diameter in the endcap region acts as a notch. The strength reduction factor was calculated to be 2.5 after evaluating Peterson's delta concept in conjunction with Neuber's equation for bending of notched bars. On the above basis, the fatigue strength of the endplate weld was determined as 22 MPa.

The endplate stress is proportional to the lateral deflection of the element. Since the outer element showed the highest value of the lateral deflection, the highest stress appeared at the web connected to outer ring of the endplate. The highest stress was 25 MPa, and was lower than the fatigue limit at the endplate web which was derived as 28 MPa by Tayal and Choo [1] using the same methodology and under the same assumptions as the fatigue strength applied to the endplate weld. The fatigue stresses at the webs connected to other rings of the endplate were far below the fatigue limit.

FUEL DEFECT ANALYSIS AT POWER CHANGES

The fuel experiences power ramps during a variety of conditions such as axial movement during normal refuelling, trip recovery and refuelling of a channel next to recently refuelled channels. The power ramps expose the fuel elements to the possibility of stress-corrosion cracking (SCC). In the Fuel Design Manual of the CANDU standard 37-element fuel bundle, the above cases are described for the assessment of fuel defect performance. The integrity of the CANFLEX fuel elements is also evaluated for the above cases with power ramps.

Analysis Method

SCC defects may occur when the operating values of element power, power-boost, and burnup exceed their allowable limit called the defect threshold. Thus to assess the likelihood of defects from this mechanism, we need to compare the operating values of the above parameters to the appropriate defect thresholds. With respect to the operating values, we have already noted that for a given bundle power the peak element ratings in a CANFLEX fuel bundle are about 20% lower than in a 37-element bundle. By itself this would tend to increase the margins to failure. Next we examine if the element diameter has a significant effect on the other part of the equation, the defect thresholds.

The FUELOGRAM model [4] is a representative correlation used to determine the defect thresholds of CANDU fuel elements due to SCC. In this model the defect thresholds are expressed in terms of operating parameters such as power ramp, ramped power and burnup. The model has the advantage of easy handling. However, since this model is empirical, its applicability is -strictly- limited to the range of its database. CANFLEX sheaths and pellets do have dimensions outside this database. In order to overcome this constraint, the SCC defect thresholds of CANFLEX fuel elements were determined by using a more recent model, INTEGRITY [5]. INTEGRITY is a semi-mechanistic model and is able to account for the effects of sheath and pellet dimensions on SCC defect thresholds [5]. It does have the disadvantage of requiring more complicated handling in that it receives necessary data from two other codes. The model is linked to the ELESTRES code [6] to get the data of fission-product concentrations and also to the FEAST code [7] to get the work density of the sheath.

To determine the SCC defect thresholds of CANFLEX fuel elements, the ELESTRES-FEAST code combination was used to determine the work densities and fission-product concentrations for many cases. Each input case had a standard power history with a single power ramp. For an input power level and a particular total burnup, the test cases consisted of power ramps ranging from 1 kW/m to 60 kW/m, in steps of 1 kW/m. By running a large array of cases in combination with the INTEGRITY model, the appropriate combinations of initial power, power ramp and burnup were determined for the cases that result in a 1% defect probability.

Defect threshold curves were obtained for both sizes of CANFLEX fuel elements. It was found that the smaller diameter of the CANFLEX fuel element leads to lower concentration of fission products, which reduces the severity of the corrosive environment. This is compensated by the higher expansion of the pellet due to subtle differences in pellet dimensions/shapes. The net result is that the 1% defect thresholds are similar for 37-element and CANFLEX bundles. This indicates that the FUELOGRAM model which has been used for the licensing calculations of the standard 37-element bundle can be used for the CANFLEX-NU bundle for the same purpose.

Reactor Physics Data

In the simulation of 600 full-power days operation of a CANFLEX-NU core, the peak bundle power was 887 kW, and the bundle-average discharge burnup was 175 MW.h/kgU. To be consistent with previous licensing assessments of CANDU 6 reactors, the high-power envelope was renormalized to a peak value of 935 kW, which is the licensed bundle power in the CANDU 6 reactors. This reference high-power envelope was used for the defect analyses for CANFLEX-NU.

The highest ramp during an 8-bundle shift was found to be 570 kW from the simulation. This increase in bundle power corresponds to an increase of 30 kW/m in the peak element linear ratings. The value of 30 kW/m was used for the CANFLEX-NU fuel defect analyses due to power ramps described in this paper.

We assessed the defect probability for CANFLEX-NU fuel following a trip recovery in a CANDU 6 reactor in a configuration with adjusters out of core. The power boosts from a trip-recovery simulation (in which a ¼ core was considered) were combined with the results from a time-average simulation. During a trip recovery, the maximum fuel power may exceed the steady-state power typical of reactivity shim operation (adjusters out of core). We defined the power boost in this case as the difference between the peak power and the steady-state power; this was found to be less than 10 kW/m in element rating.

Results and Discussions

Power Ramp Due to Refuelling

Figure 3 compares the reference high-power envelope with the FUELOGRAM defect threshold for increased power, and also compares the highest power ramp of each element with the FUELOGRAM defect threshold for power increases. For fuel failure probability to exceed 1%, both threshold curves must be exceeded. No defects were predicted for CANFLEX fuel.

Trip Recovery

Figure 4 shows the prediction of defect probability during trip recovery in a CANDU 6 reactor. Curves for 1% and 2% defect probability are shown; the former is also called the defect threshold. The power increase was considered to be the power overshoot from the previous steady-state power. To assess the fuel defect probability, the ramped power was determined by adding 10 kW/m uniformly to the nominal design power envelope of CANFLEX fuel over the whole burnup range. Since the nominal design power envelope bounds all steady-state powers of the bundles, the uniform addition of 10 kW/m is conservative. With this conservatism the defect threshold for ramped power is exceeded slightly in the burnup range of 80-150 MW.h/kgU.

For fuel defect to occur, both the ramped-power and power-boost thresholds need to be exceeded. Considering the power-increase versus burnup curves in Figure 4, in almost all individual bundles the power boost is the variable that controls the defect probability. The plots of power increase vs. burnup show that very few bundles in the core during the trip recovery would be over the defect threshold, and in fact only slightly over this threshold.

Previous simulations of trip recovery have shown that in a CANDU-6 reactor the maximum power-boost in 37-element fuel is 12 kW/m, and the fuel performs well. In comparison, the CANFLEX fuel experiences a smaller power-boost (maximum of 10 kW/m), and hence is at even lower risk of SCC defects. Considering that our assessment is conservative and yet the failure probability is very low, the performance of CANFLEX fuel is acceptable.

Normal Refuelling of a Channel next to Recently Refuelled Channels

In the 8-bundle shift fuelling scheme, the worst-case bundle from the standpoint of power-ramp defect predictions is a bundle that starts in position 1 and is moved to position 9 in a normal refuelling operation, the bundle then being subjected to a further power ramp. This power ramp would be due to refuelling in a neighbouring channel; for example, a normal refuelling is done in one channel and is followed by an abnormal refuelling to remove defective bundles from the neighbouring channel. Because of the normal and abnormal refuelling in neighbouring channels, the bundle that starts in position 1 and is moved to position 9 will be subjected to a 25% increase in bundle power. Even though the peak bundle power reaches 1,000 kW and the largest power ramp is 38 kW/m, no defect was predicted; see Figure 5.

SHEATH COLLAPSE INTO THE CONCENTRATED AXIAL GAP OF THE CANFLEX FUEL ELEMENT

An axial gap is provided to accommodate the weld upset generated by the welding of the sheath to the endcap and to accommodate the differential axial expansion between the pellet stack and the sheath. A simple calculation shows that an axial gap will be maintained following axial expansion of the pellet stack. Therefore, it is necessary to evaluate the potential for sheath collapse into the concentrated axial gap due to external pressure. This analysis is also required for the Fuel Design Manual.

Instantaneous Collapse

A statistical treatment method which is based on Donnell's model plus the Monte Carlo method has been used in licensing calculations of the CANDU standard fuel elements to analyse the instantaneous collapse of the sheath into the axial gap in an element. This statistical model was also used for the same purpose in evaluating the CANFLEX fuel element design.

The analysis, using parameters representative of CANDU 6 CANFLEX fuel, predicts that a 0.01% probability of collapse of the sheath occurs at a pressure of 23.6 MPa for the small-diameter element and 21.6 MPa for the large-diameter element (see Figure 6). These are much higher than the coolant pressure in the CANDU 6 reactor. These predictions were compared with the finite-element analysis results, and were found to be more conservative.

Creep Collapse

The FEAST code [7], which analyses the stresses and strains in the structural material by the finite-element method, was used to evaluate the sheath collapse into the axial gap in the element subjected to high external pressure and temperature. The MATPRO model [8] for Zircaloy creep was used, and the analysis was performed for the case of 10 000 h. The analysis showed that no additional deformation of the sheath in the axial gap zone occurred due to creep for 10 000 h after loading. This result qualitatively indicates that creep collapse of the sheath into the element would not occur.

FATIGUE ANALYSIS OF THE ELEMENTS SUBJECTED TO POWER CYCLES

For licensing in Korea, the CANFLEX fuel bundle is required to withstand many hundreds of power cycles. Hence we assessed if the repeated expansion and contraction of the pellet could possibly lead to sheath fatigue.

For the analysis all bundles were assumed to experience 1500 power cycles in the reactor. Actually, this is 10 to 60% higher than the maximum number derived from the expected in-reactor residence times of the bundles. In reality, inner-core bundles experience comparatively smaller number of power cycles but at higher power, while outer-core bundles experience comparatively larger number of power cycles at lower power. But, in this analysis, all bundles were assumed to be operated with the nominal design power envelope. The power cycles were considered to be composed of 1246 daily cycles, 250 weekly cycles, 1 nominal start-up after a poison-out shutdown, 1 trip recovery after 30 minutes, 1 poison-prevent recovery and 1 shim operation. For daily and weekly cycles, the power was assumed to cycle 100%-60%- 100% intermediate power. For reactor start-up cases, the full power was assumed to be recovered at the rate of 1%/s. In the shim operation, the full power was assumed to be recovered from 50% to 100%.

For each transient, the fatigue damage of the element was obtained from O'Donnell-Langer model. That is, the maximum alternating strain in the sheath was calculated by the ELESTRES code, and this value was adapted to the O'Donnell-Langer model to obtain the permitted number of cycles. By comparing the permitted number to the design number of cycles, a fatigue damage ratio was obtained.

The cumulative fatigue damage was obtained by summing the fatigue damage ratios from all the transients. For the CANFLEX-NU fuel bundle, the cumulative fatigue damage was obtained as 0.02 for both inner and outer elements. These are very low compared with the conventionally accepted limiting value.

CONCLUSIONS

Some design considerations that are not assessed by experiments but which should be evaluated from the standpoint of fuel integrity were analysed with the use of well-established analytical methods with reasonable support from similar experiments or applicable experience. The following conclusions were reached from these analyses:

1. Fatigue failure at the endplate weld and the endplate web due to lateral vibration of fuel elements subjected to axial flow of coolant in CANDU 6 reactors will not occur in the CANFLEX-NU fuel design.

2. SCC defects due to various kinds of power ramps have a low probability of occurring in CANFLEX fuel elements and will be lower than 37-element bundles.

3. Sheath collapse into the concentrated axial gap in CANFLEX fuel elements will not occur. It is also expected that there will be no additional deformation of the sheath in the axial gap zone due to creep.

4. Fatigue failure of the element subjected to a significant number (1500) of power cycles will not occur.

ACKNOWLEDGEMENT

The authors thank Mr. P.G. Boczar of AECL for his valuable suggestions during the preparation of this paper.

REFERENCES

[1] TAYAL, M, and CHOO, C.K., "Fatigue Analysis of CANDU Nuclear Fuel Subjected to Flow-Induced Vibrations", AECL report AECL-8331, 1984.

[2] ROARK, R.J. and YOUNG, W.C., "Formulas for Stress and Strain", McGraw-Hill Book Company, Fifth Edition, 1975.

[3] PAIDOUSSIS, M.P., "The Amplitude of Fluid-Induced Vibration of Cylinders in Axial Flow", AECL report AECL-2225,1965.

[4] HARDY, D.G., WOOD, J.C. and BAIN, A.S., "CANDU Fuel Performance and Development", AECL report AECL-6213, 1978.

[5] TAYAL, M., HALLGRIMSON, K., MACQUARRIE, J., ALAVI, P., SATO, S., KINOSITA, Y., and NISHIMURA, T., "INTEGRITY: Semi-Mechanistic Model for Stress Corrosion Cracking of Fuel", AECL report AECL-10792, 1994.

[6] TAYAL, M., "Modelling CANDU Fuel under Normal Operating Conditions: ELESTRES Code Description", AECL report AECL-9331, 1987.

[7] TAYAL, M., "FEAST: A Two-Dimensional Non-Linear Finite Element Code for Calculating Stresses", AECL report AECL-8763, 1986.

[8] "MATPRO-Version 10, A Handbook of Materials properties for Use in the Analysis of Light Water Reactor Fuel Rod Behaviour", NUREG/CR-0497.

[Store: WORD\h\Canflex\Simpaper_971024]

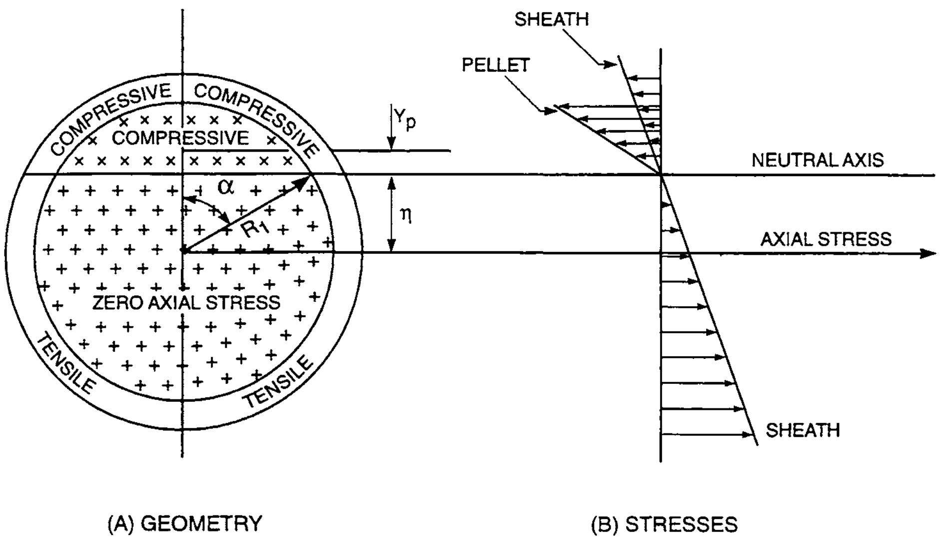

Figure 1 Geometric Model of the Fuel Element as a Composite Beam Comprising of the Sheath and the Pellet

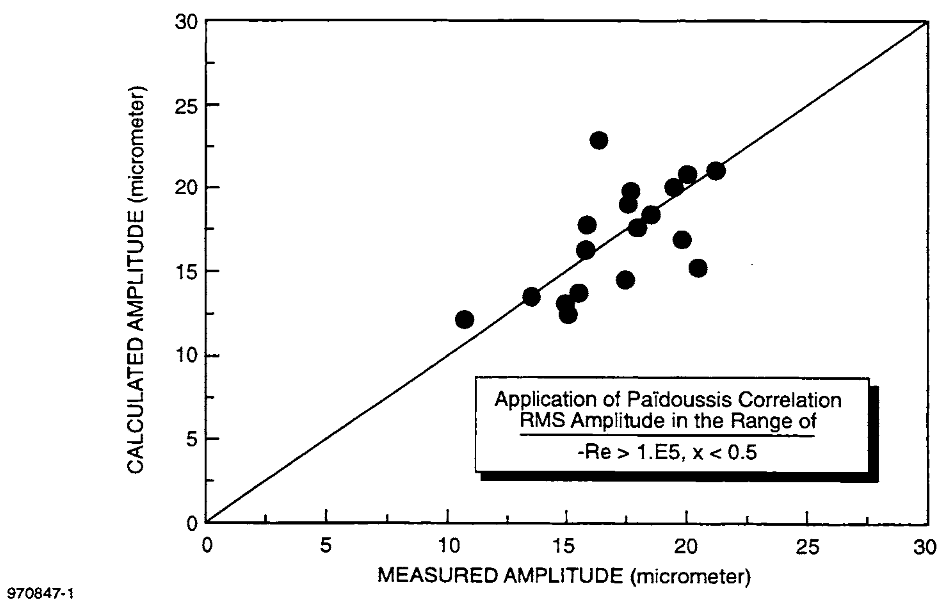

Figure 2 Applicability of the Païdoussis Correlation to the CANFLEX Fuel Elements for Calculating Vibration Amplitude of the Element

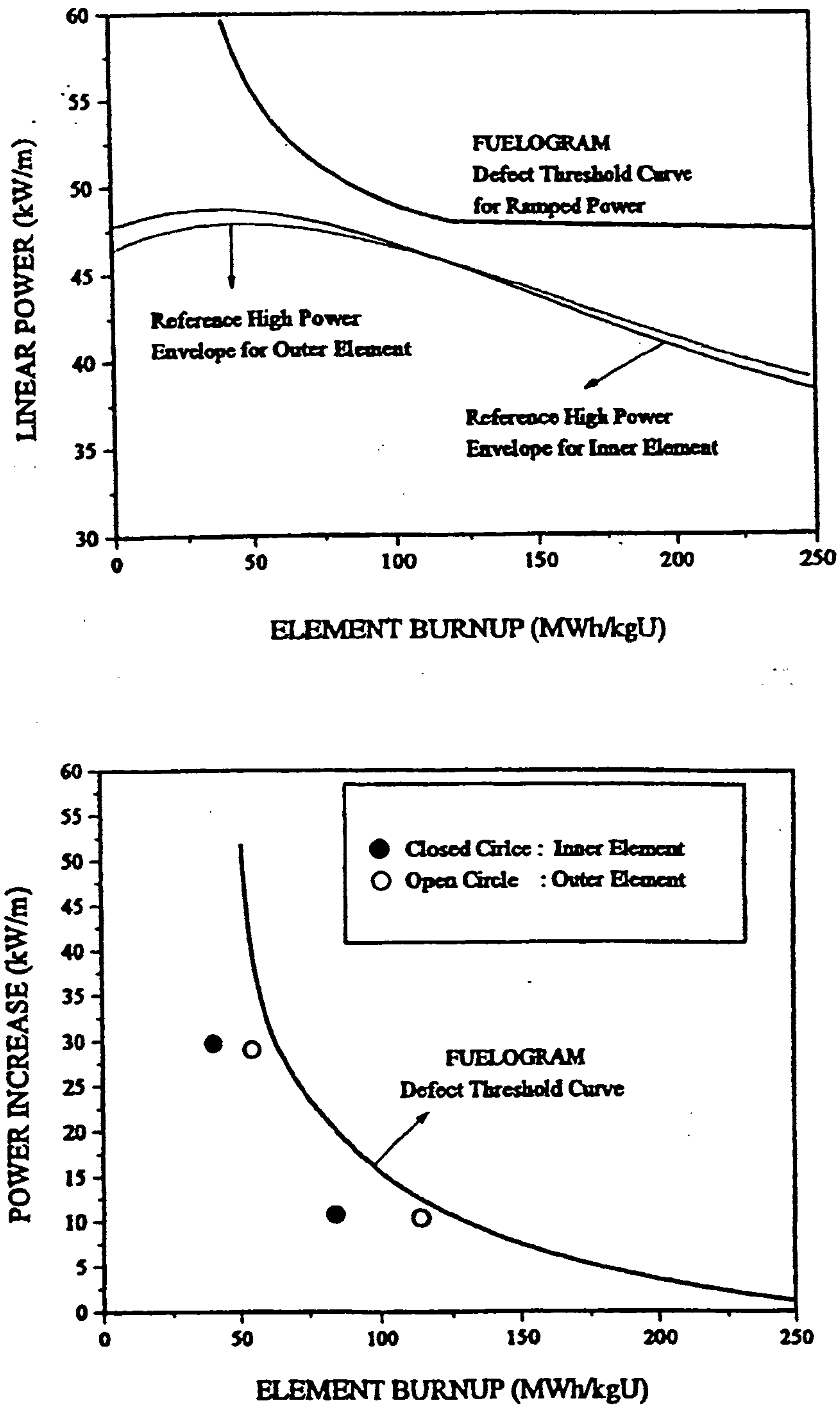

Figure 3 Defect Analysis of CANFLEX-NU Elements in Terms of FUELOGRAM Defect Threshold Curves for the Case of Normal Refueling.

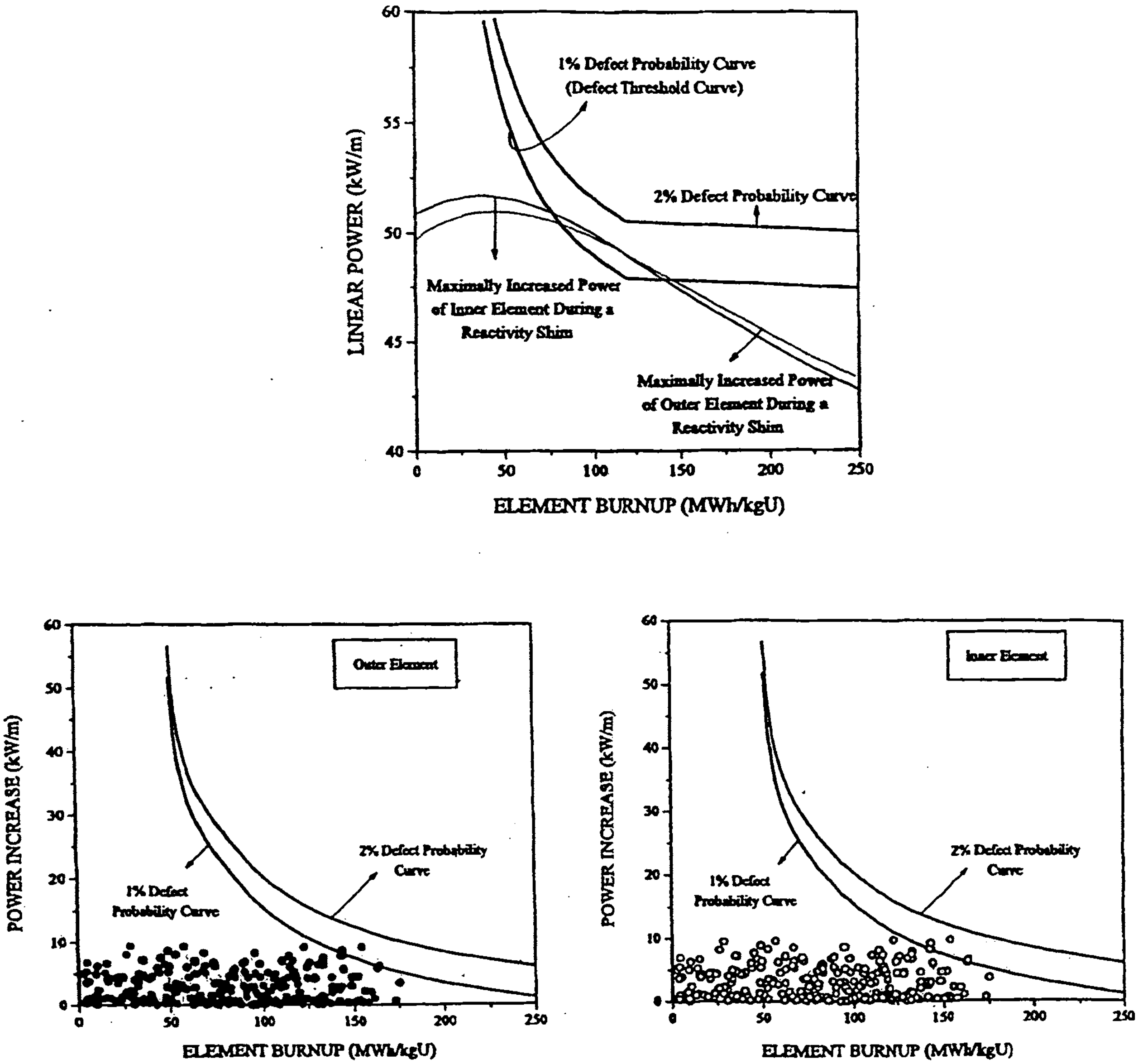

Figure 4 Defect Analysis of CANFLEX-NU Elements in Terms of FUELOGRAM Defect Threshold Curves for the case of Trip Recovery.

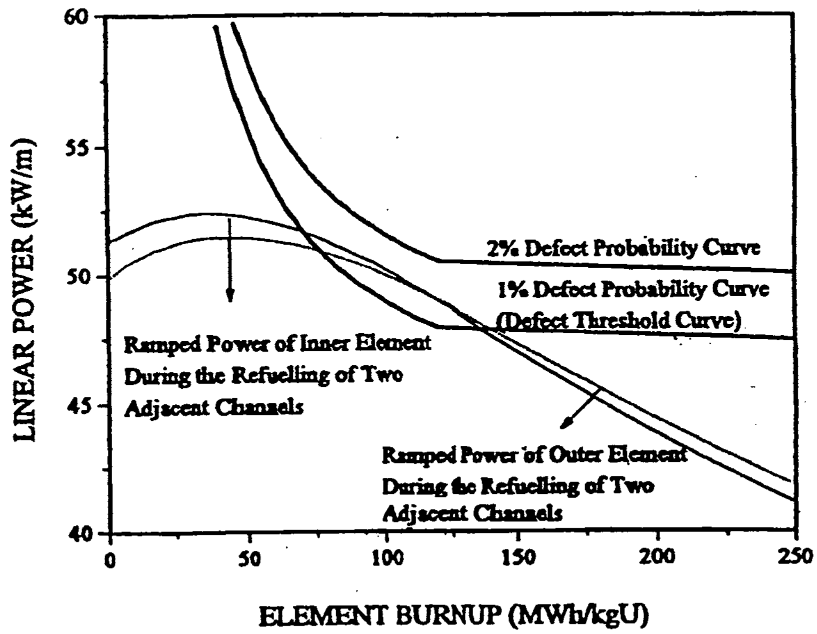

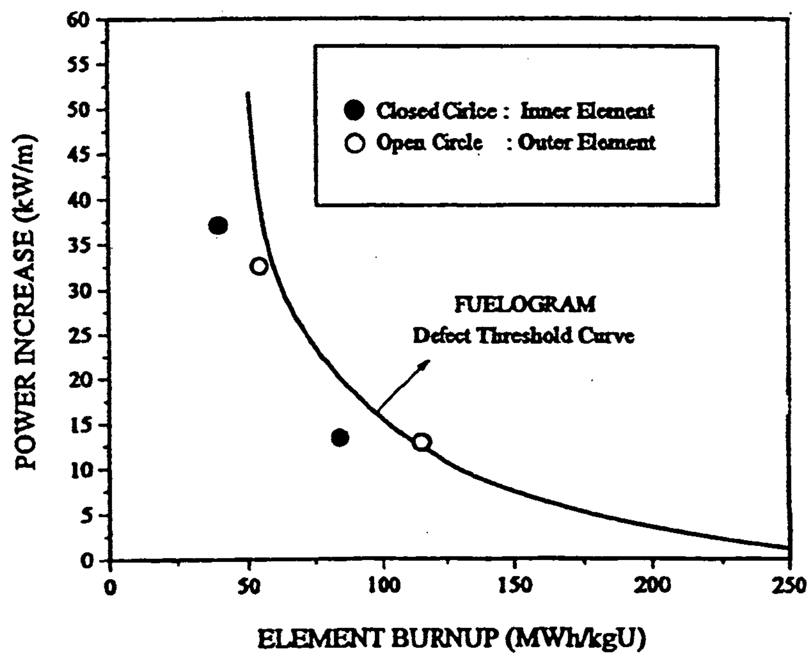

Figure 5 Defect Analysis of CANFLEX-NU Elements in Terms of Fuelogram Defect Threshold Curves for the Case of Normal Refuelling of a Channel Next to Recently Refuelled Channels

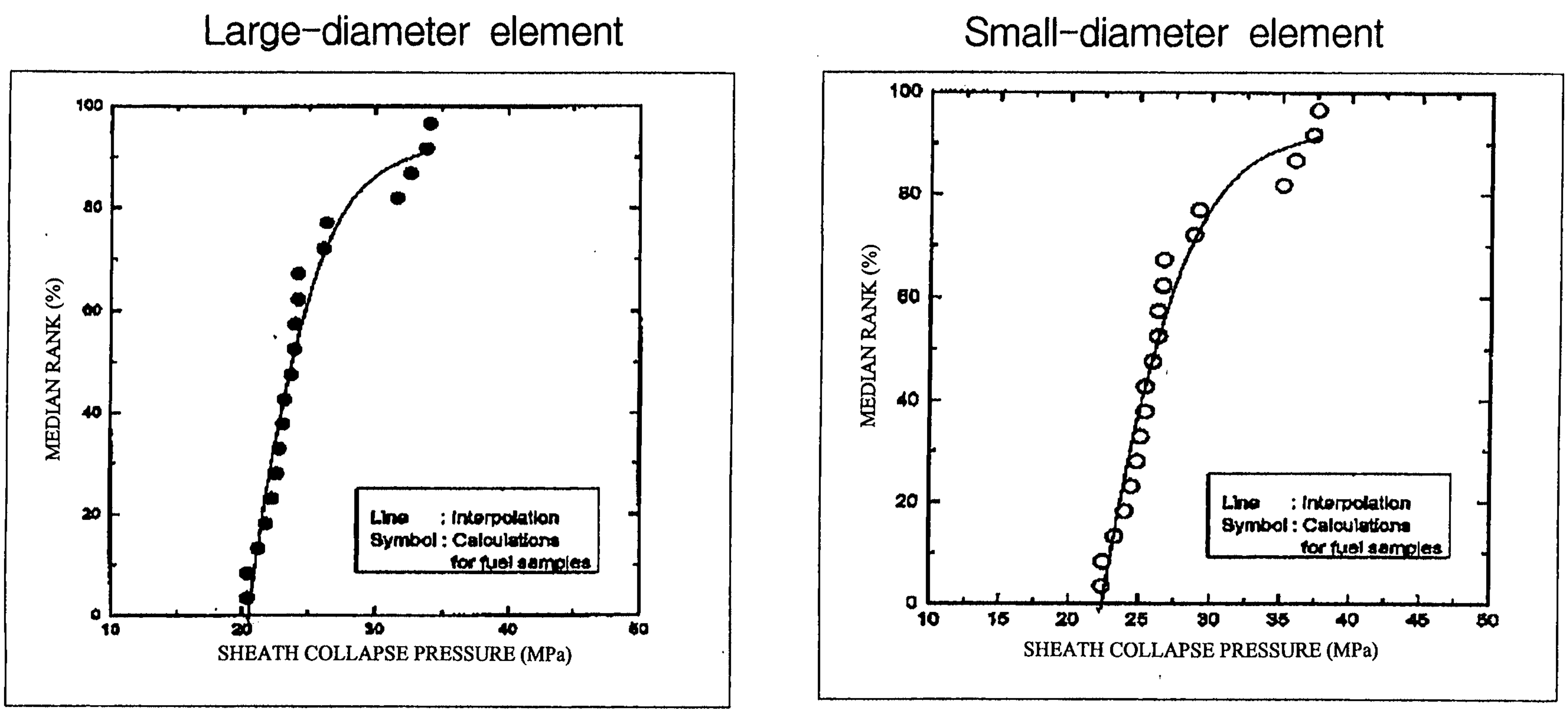

Figure 6 Sheath Collapse Pressure into the Concentrated Axial Gap.